9th International Conference on Probabilistic Methods Applied to Power Systems
KTH, Stockholm, Sweden – June 11-15, 2006

Statistical Wind Speed Interpolation for Simulating Aggregated Wind Energy Production under System Studies

M. Gibescu, B.C. Ummels and W.L. Kling
Electrical Power Systems Laboratory
Delft University of Technology
Delft, The Netherlands
Email: m.gibescu@ewi.tudelft.nl

Abstract— **In this paper we present a statistical interpolation method to generate a time series of system-aggregated wind power production values that can be used as an input to system operations planning tools such as Unit Commitment (UC) and Economic Dispatch (ED). We use historical wind speed data measured at several locations, in order to estimate average wind patterns and express the covariance between locations as a function of their distance. Then, for a new set of locations where wind parks are planned, we create wind time series for the study period such that the spatial correlation between the sites is taken into account. Depending on the system under study, this may be of specific importance due to the concentration of areas with favorable wind conditions, resulting in strong correlations between wind park outputs. These cross-correlations are essential when evaluating system adequacy and security in planning mode, in the presence of large-scale wind power. The resulting aggregated wind power time series are finally fed into the UC-ED module to help evaluate the amount of total system reserve required to maintain an adequate level of reliability. The method is applied to a simplified version of the Dutch power system.**

I. Introduction

As power systems have to accommodate an increasing amount of renewable generation, which is often random and hence non-dispatchable, the need for employing probabilistic methods in planning of operations becomes more apparent. Such methods exist already, e.g. to deal with the random nature of generating unit outages and with load forecasting uncertainties [1]. Established measures of system reliability are loss-of-load expectation (LOLE) and expected energy not served (EENS) [2]. In a Unit Commitment and Economic Dispatch framework (UC-ED), reserve is added to each time period of the study to decrease EENS below a given threshold, whose value is often dictated by financial considerations.

A natural choice for extending this framework is to treat wind generation as negative load and solve the UC-ED problem using the average wind power values for each study period. As a final step, the wind power production uncertainty can be incorporated into the EENS calculation. This method is also applicable in a market situation: EENS can then indicate, to a Load-Serving Entity with conventional as well as wind production units in its portfolio – instead of the expected unserved energy – the overall amount of energy imbalance that it will expect to purchase from the System Operator.

In the case when wind is present on the system, a larger amount of reserve would have to be allocated from the remaining conventional units in order to achieve the same level of reliability (i.e. equal EENS with the case when the entire load was served by conventional generation only). The remaining question is how that uncertainty in total wind production can be quantified. Current methods for creating (Weibull) probability distributions of wind speeds are not applicable, as they can only give an idea of the expected wind energy production at a particular geographic location over long periods of time, such as yearly outputs (WAsP is a typical software tool that can be used for this purpose).

Capacity adequacy in the presence of wind energy is investigated in [3] via a Monte Carlo approach, and the contribution of wind energy conversion systems to generation system reliability is quantified. The classic probabilistic approach for determining the operating reserve in the Pennsylvania-Jersey-Maryland pool is modified in [4] to account for both the random nature of wind power output and the unavailability of wind parks. Reference [5] focuses on quantifying the reserve requirement for systems with a large degree of wind penetration based on several scenarios for operating conventional generation and two different wind forecast horizons. Reference [6] also investigates the impact of wind power on the required level of three types of system reserves under central dispatch. However, most of these studies use synthesized wind time series as an input to the analysis, rather than series based on actual measurements, as presented in this work. Sophisticated meteorological models for geographical interpolation of wind speeds, such as the Internal Boundary Layer, are discussed in [7]. Unlike our purely statistical method, such models require accurate knowledge of the roughness of the terrain and also wind direction information.

With increasing penetration, wind power will have a significant impact on reserve levels (due to limited predictability of wind) and ramp rate requirements for conventional units (as a result of aggregated load and wind power variations) and therefore on the resulting unit commitment schedules.

This research focuses on the generation system alone. It is assumed that no congestion will occur in the transmission system, and hence line flow constraints are ignored. Independence is assumed between the three categories of random variables: conventional unit outages, load uncertainties, and total wind production levels. Generation mix by technology is consistent with the anticipated wind and conventional generation developments in the next decade in Western Europe. Assumed park locations and computed wind speeds are based on data from the Netherlands.

II. Wind Speed Measurements

Wind power production was modelled using weather data and wind turbine power-speed curves. Wind speed data have been obtained from the Royal Dutch Meteorological Institute (KNMI). The data set contains 10-minute wind speed averages with a resolution of 0.1 m/s for 18 locations in the Netherlands (9 onshore, 3 coastal, and 6 offshore) measured between June 1, 2004 and May 31, 2005. This historical wind speed data is used to estimate average daily wind patterns and to express the covariance between locations as a function of their distance. Then, for a new set of locations where wind parks are planned, wind time series for the study period are created such that the spatial correlation between the sites is taken into account. This is required because wind energy production units will be concentrated in areas with favorable wind conditions, hence their outputs may be strongly correlated. These cross-correlations are thus essential when evaluating system reserve and ramp rate requirements in operations planning mode.

For each of the 18 locations we first plot the sample variance versus the sample mean in figure 1. We note a clear linear relationship between the two (the so-called heteroscedasticity). To suppress it, we apply a variance stabilizing transformation ([8], section 9.2), and from here onwards we will work with the natural logarithm of wind speed. This will simplify the regression model presented later in this section by allowing for a single, mean-independent variance of the interpolated logarithm wind speeds valid for all locations.

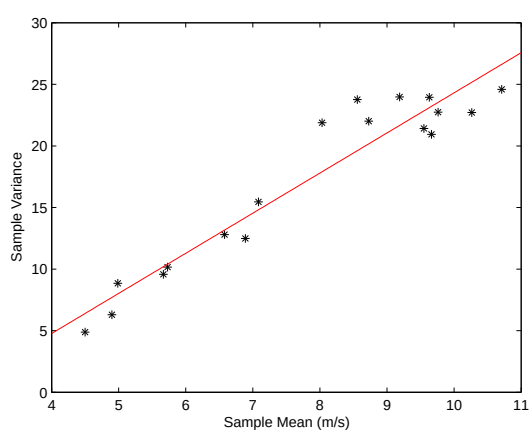

Fig. 1. Mean-Variance Relation for Wind Speed Measurements

Let $W(z,t)$ be the log wind speed at a location $z = (x, y)$ in cartesian coordinates and time $t = (d, k)$ defined by day of the year d and time of day k. We consider a general model:

$$W(z,t) = \mu(z,k) + \varepsilon(z,d,k), \tag{1}$$

where $\mu(z,k)$ is a deterministic variable representing the daily wind pattern by location and $\varepsilon(z,d,k)$ is a zero-mean random process representing the variations around the daily mean. We will pay special attention to the covariance structure of this random process, because it is not realistic to assume that the variations of wind speed about the daily mean are independent across space, especially for small geographical areas.

In figure 2 we plot the average daily wind pattern for each of the 18 measured locations:

$$\hat{\mu}(z,k) = \sum_{d=1}^{365} W(z,d,k)/365, \tag{2}$$

for $z = 1, 2 \ldots, 18$, and $k = 1, 2 \ldots, 24 \times 6$. This plot suggests that our model should contain a daily effect that varies smoothly with geographic location. Measurements sites on land display a typical unimodal pattern with a maximum around midday, while sites offshore have a much flatter daily profile, and the coastal locations fall somewhere in between.

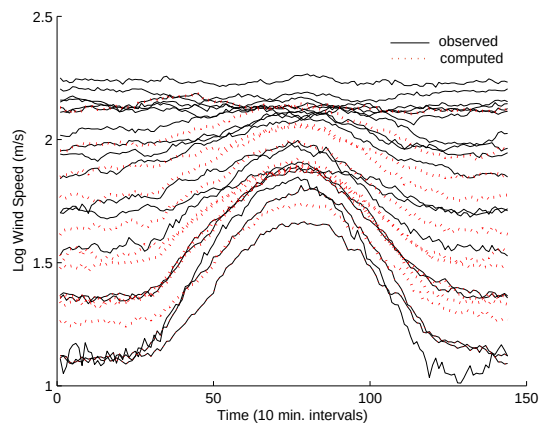

Fig. 2. Daily Wind Speed (m/s) Pattern for Measured & Estimated Locations

We now have the values for the mean log wind speed $\mu(z,k)$ at the 18 measurement locations. To obtain the mean log wind speed at a different location we would need to know its coordinates $z = (x, y)$ and apply a linear spatial interpolation for locations within the convex hull formed by the measurement sites, or alternatively, a nearest neighbor interpolation for locations outside the convex hull. The result is shown via the dotted lines in figure 2.

In order to estimate the random component $\varepsilon(z,t)$, we will also require a model for the covariance $\mathrm{Cov}(\varepsilon(z_1,t), \varepsilon(z_2,t))$ between two locations z_1 and z_2. Figure 3 shows the covariance between the log wind speed at pairs of locations versus the distance between them. Looking at this plot, and taking into account that the covariance should vanish at very large

distances, it seems reasonable to model it via an exponential decay:

$$\mathrm{Cov}(\varepsilon(z_1,t),\varepsilon(z_2,t)) = \alpha \mathrm{e}^{-\beta||z_1-z_2||}, \tag{3}$$

where $||z_1 - z_2||$ denotes the Euclidean distance between the two locations.

We can estimate the parameters α and β by a least squares fit. The fit is also shown in figure 3, where α = 0.32, and $1/\beta$ = 392.36 (km). The latter term is also known as the *characteristic distance* or *decay parameter*. If we translate the parameters of this decay fit from logarithmic to pure wind speeds, and look at correlation coefficients rather than covariances between location pairs, we obtain a value of 610 km for the characteristic distance. This value is in line with the 723 km reported in [9] (chapter 6), which is based on measurements from 60 locations spread throughout the European Union, and the 500 km reported in [10], using Danish data alone.

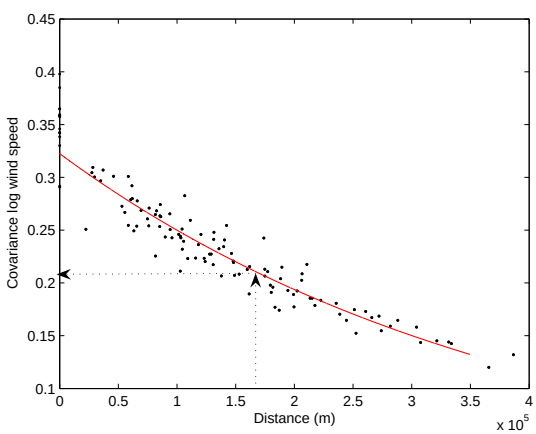

Fig. 3. Covariance versus Distance for 18 Measurement Sites

Using this exponential decay fit we can now estimate a vector of covariances between a computed location and all the measured locations.

III. Wind Speed Spatial Interpolation

A. Method

We want to use the measurement data to estimate a time series of wind speeds at a new location given its coordinates, while taking into account the spatial correlations among wind speeds for the same moment in time. The measured wind speeds generally refer to a sensor height, which may differ per location. To convert to a chosen (common) hub height one can use the methods provided in [11] or [12]. References [11] and [12] both use the logarithmic vertical wind speed profile to estimate wind speeds at heights other than the sensor height. Whereas in [11] the local roughness length is employed, which is difficult to determine for onshore locations, in [12] this need is eliminated. Instead, two location-dependent parameters are used: friction velocity and the average Monin-Obukhov (or Stability) Length. The sample wind speed standard deviation provides an estimate of the friction velocity and originates from the measured wind speed data set. If this standard deviation is not available *and* the location is offshore, then the friction velocity may be estimated directly from the vertical wind speed profile. Estimating the actual Stability Length by its average is warranted by the fact that, averaged over a long period of time, the vertical wind speed profile is stable [13].

Our goal is to interpolate wind speeds at several locations where we do not have any measurements. More precisely, we will estimate the conditional distribution of wind speeds at those locations, given wind speeds at locations where we do have observations. Choose a time t and suppose that we want to know the conditional distribution of the wind speed at n locations $z_1, z_2, \ldots, z_n$, given observed wind speeds at m locations $z_{n+1}, z_{n+2}, \ldots, z_{n+m}$.

Consider two random vectors, the computed and observed wind speeds:

$$X^{(c)} = [W(z_1,t), W(z_2,t), \ldots, W(z_n,t)]$$
$$X^{(o)} = [W(z_{n+1},t), W(z_{n+2},t), \ldots, W(z_{n+m},t)],$$

and define X as the concatenation of the two vectors:

$$X = \begin{pmatrix} X^{(c)} \\ X^{(o)} \end{pmatrix}.$$

Now suppose that X has a multivariate normal distribution with mean μ and covariance matrix Σ. We can estimate μ_i by the appropriate daily average. Similarly, we can estimate σ_{ij} by the sample covariance when available, and by using (3) otherwise. We write

$$\mu = \begin{pmatrix} \mu^{(c)} \\ \mu^{(o)} \end{pmatrix}, \qquad \Sigma = \begin{pmatrix} \Sigma_{cc} & \Sigma_{co} \\ \Sigma_{oc} & \Sigma_{oo} \end{pmatrix}.$$

If $\det(\Sigma_{oo}) > 0$, then conditionally on $X^{(o)}$ the distribution $X^{(c)}$ is again normal (c.f. [8], section 1.6) and given by:

$$\mathcal{N}(\mu^{(c)} + \Sigma_{co}\Sigma_{oo}^{-1}(X^{(o)} - \mu^{(o)}), \Sigma_{cc} - \Sigma_{co}\Sigma_{oo}^{-1}\Sigma_{oc}). \tag{4}$$

We define our interpolant $\hat{X}^{(c)}$ as

$$\hat{X}^{(c)} = \mathbb{E}(X^{(c)} \mid X^{(o)}) = \mu^{(c)} + \Sigma_{co}\Sigma_{oo}^{-1}(X^{(o)} - \mu^{(o)}). \tag{5}$$

The above expectation is the best estimate for $X^{(c)}$ given the observations $X^{(o)}$ under our assumption of normality.

We have assumed that X (logarithm of wind speeds) has a multivariate normal distribution for mathematical convenience only. Consequently, we assumed that the wind speeds would follow log-normal distributions. In reality, the marginal distributions of wind speeds appear to be better described by Weibull distributions. However, our results show that the residuals $X^{(c)} - \hat{X}^{(c)}$ do seem to follow a multivariate normal distribution with mean 0 and covariance matrix

$$\Sigma_{cc} - \Sigma_{co}\Sigma_{oo}^{-1}\Sigma_{oc}. \tag{6}$$

This is very fortunate indeed, as it will allow us – among other things – to construct confidence intervals for any function of $X^{(c)}$ that we might be interested in, such as wind power output for given speed (see section IV-A).

B. Cross-Validation

The method was verified by removing one location at a time from the n-site measurement set and using the remaining n-1 measurement sites to estimate it. The estimation error is itself a random variable, defined as the difference between estimated and measured wind speed: $F_i = \hat{X}_i - X_i$, for $i = 1 \ldots n$. This vector of random variables, each with a sample size of $365 \times 24 \times 6$ data points, is characterized by a vector of sample means and sample standard deviations. The sample mean is zero for an unbiased estimate. The results for the standard deviation of the estimation error for the $n = 18$ sites used in this study are shown in figure 4. The overall average standard deviation of the error is about 1.2 m/s. The two locations that exhibit the largest errors are the meteorological stations of F3 and K13 (3 and 2.5 m/s standard deviation respectively), which are situated offshore in isolated locations and therefore have quite distinct behavior from the rest of the measurement set.

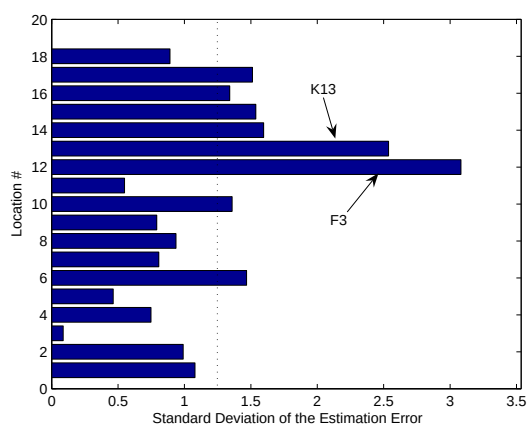

Fig. 4. Standard Deviation (m/s) of the Estimation Error for 18 Locations

C. Interpolation Results

An example of the first week speed profile for a number of measured and estimated sites is shown in figure 5. The top subplot shows a week's worth of measured wind speeds for two locations selected from the measurement set, which are the *most* and the *least* correlated with the two computed time series shown in the bottom subplot. This picture illustrates the idea of simultaneous variation among highly correlated sites.

IV. Application to System Studies

The interpolation method described in section III is applied to a simplified model of the Dutch power system as it may look by 2012. This system has a peak load of 20.5 GW and an installed capacity of around 23 GW (excluding wind power), out of which about 20% is connected at the distribution level and hence not available for central dispatch. In addition, about 55% of all units are Combined Heat and Power (CHP), which exhibit somewhat less flexibility than other technologies due to their heat demand schedules, in combination with constraints

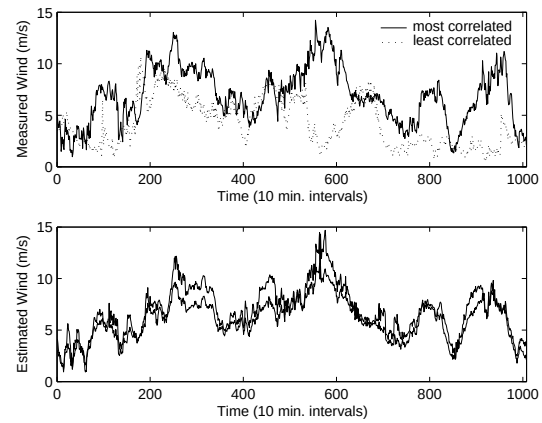

Fig. 5. Estimated and Measured Speed Profiles for One Week

coupling their heat and electrical power outputs. The UC-ED simulation is done sequentially for 15-minute intervals over a study period of one year. The objective is fuel cost minimization, while meeting the load and satisfying reserve and ramp rate constraints. The decision variables are the status and MW outputs of all dispatchable units in the system. The simulations are carried out with load served by conventional generation only as base case, and then for 8 GW installed wind capacity,. This would cover about 22% of the projected yearly national electricity consumption. The setup of the UC-ED simulations carried out for this system study is described in more detail in [14].

A. Conversion to Wind Power Output

For each of the projected locations, wind turbines have been modelled using "smooth cut-out" power-speed curves to compute the power output for any given wind speed. The curve used is shown in figure 6 (see example at *http://www.enercon.de*).

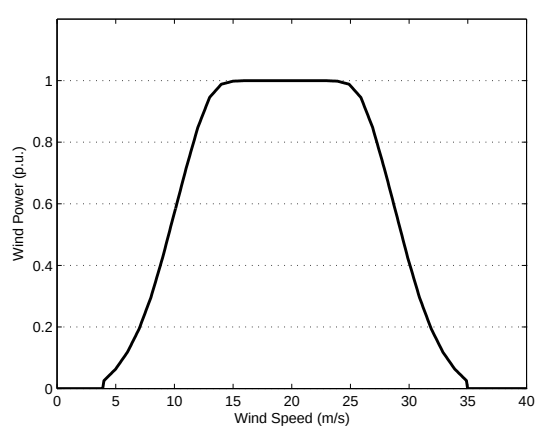

Fig. 6. Aggregated Wind Speed to Power Conversion Curve

In the previous section we have described a method for

interpolating the logarithm of wind speeds. To obtain ordinary wind speeds, we first exponentiate. If we assume that all the turbines in a park are perfectly correlated, then we can multiply the power output of a single turbine by the number of turbines to get the total output of the wind park. This computation is not entirely accurate as it ignores park effects, such as spatial smoothing and wake. However, the "smooth cut-out" speed-power curve approximates the offsets for true cut-out speed among various turbines in the park and results in a somewhat less dramatic aggregated output changes as the wind averages oscillate above and below the threshold value for a single turbine. Wake effects depend on both wind direction and wind park lay-out; as both are unknown, wake effects are not considered here.

Via a Monte Carlo simulation we can determine the extent to which estimation errors in wind speed of the order of magnitude described in the section III-B will translate into errors in estimating the aggregated system-wide wind power output. We sample from a multivariate, normally distributed logarithm wind speed error function, with mean 0 and co-variance matrix given by (6). We add this random error to our estimated log speeds, exponentiate, and pass it through the power-speed curve (fig. 6). We then sum up the wind outputs per location and finally average the results to obtain the system-wide distribution of total wind power production. It should be noted that the sample mean of the wind production obtained via this simulation is actually an unbiased estimate for that particular time point. This mean, together with the associated point-wise 90% confidence band, is shown in figure 7, for a week's worth of 10-minute time intervals. This graph shows that, with 90% confidence, the true aggregated wind power output will fall somewhere in the range delimited by the higher and lower black time-series. The standard deviation of the wind power production (conditional on the observed wind speeds) increases with the output to be estimated, ranging from 16 to 1061 MW. The largest uncertainty occurs when estimating outputs that approach the full installed capacity of 8000 MW. The average standard deviation comes out to 500 MW, which translates to about 20% of the amount to be estimated.

B. Estimation of Wind Variability

Given locations and installed powers for future wind parks, the estimation method in section III can be used in combination with the aggregated speed-power curve presented in figure 6 to compute system-wide average wind power generated per 15 minute time interval for the duration of an entire year. (The change from 10 to 15 minute averages was required by the design of the Dutch energy market.) The total installed wind power chosen for the simulations was approximately 2 GW onshore and 6 GW offshore. By differentiating the wind power series we obtain an estimate of the variability of wind production across 15 minute time intervals. Similarly, an estimate of system load variability can be constructed. The sorted load variations during the study year are shown in

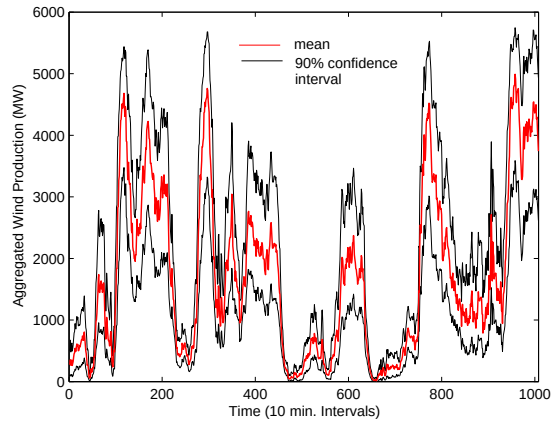

Fig. 7. Estimate of Total Wind Power with Confidence Interval

figure 8, together with the (correspondingly sorted) aggregated, load minus wind power variations time series. This graph shows that the variations in load and wind are uncorrelated, an assumption which will be used in the following section. The order of magnitude of the aggregated load and wind power variations is roughly twice that of load variations alone, and its maxima may occur equally in either positive or negative direction. This quantity and its sign are of special interest, as simultaneous load and wind variations must be balanced by the remaining conventional generation units via up or down-ramping of their outputs.

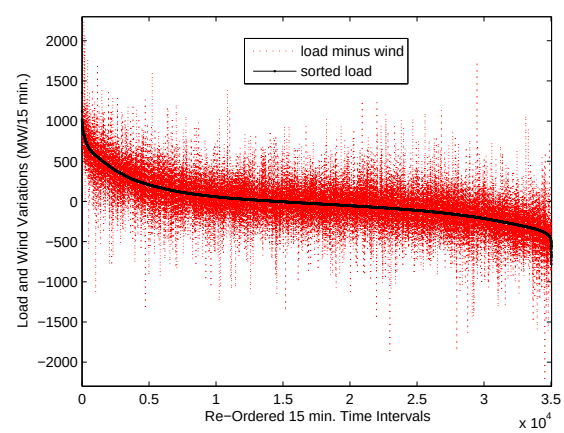

Fig. 8. Variations in Load and 8 GW Aggregated Wind per 15-Min. Intervals

C. Reserve and EENS

System reserve is allocated among on-line generators to account for equipment outages and uncertainties in load and wind forecast errors. Only spinning reserve from conventional units (i.e. no fast start-up, or electricity storage) was considered in this study. It is quite obvious that the higher the forecast uncertainty, the larger the amount of reserve needed to achieve the same reliability level. In this subsection, we

use a simulation method to sample from the joint, discrete distribution of generating capacity outages and the continuous distribution of net (load minus wind) forecast errors, to arrive at a value for LOLE per 15 minute time interval. The value of LOLE is dependent on both the system reserve and the standard deviation of the prediction errors. The classic LOLE, EENS and COPT (Capacity Outage Probability Table) concepts employed are described in [15].

1) Load Served by Dispatchable Generation Only: Typically short-term load forecasting errors are normally distributed with mean zero and standard deviation around 2.5-3% [16] (chapter 2). We will assume a conservative value of 4% in this study.

2) Some Load Served by Wind Power: An often quoted error estimate in the wind power prediction error, day-ahead, for a single location, is about 15% of the installed capacity (see [17] and the excellent survey in [18]). Moving on from single-site prediction, we would like to mention [19] and [20] on forecast error aggregation per multiple sites. Based on the RMSE (root mean-square error) reduction as a function of the diameter of the area where wind parks are installed provided in [20], we will assume a 0.25 reduction in the aggregated offshore wind forecast error (corresponding to an area of about 200 km. diameter) and a 0.50 error reduction for the onshore forecast error (corresponding to a larger area, of about 400 km. diameter). The idea of convoluting load and wind forecast error probability density functions – assumed gaussian and independent – for use in system reserve estimation appears for the first time in [21].

For the onshore and offshore installed wind capacities chosen in this study, the resulting standard deviation of the wind power forecast error is then:

$$0.15 \times (0.75P_{offshore} + 0.5P_{onshore})$$

which comes to 825 (MW) or about 10%. This value is in line with the 8-9% quoted for the day-ahead Nord Pool electricity market in [22]. The day-ahead prediction horizon – i.e. 12-36 hours ahead of real-time – is important since this is when the planning of operations for next day is performed. This time lead also coincides with the closure of the Day-Ahead Market.

As part of a sensitivity analysis, the impact of larger wind forecast errors, with standard deviations of 20% and 40%, were also investigated. A half week's worth of 15 minute unit commitment time periods was analyzed. The wind production time series developed in the first half of this paper were used as an input to the UC-ED software. The program uses a simple minimum reserve criteria, i.e. the size of the largest equipment outage (conventional unit or import interconnector). This criteria is based on traditional utility practices and is independent of the level of wind penetration, or the wind power forecast accuracy. The results are shown in table I, where both Reserve energy and EENS are expressed in percentages of the energy served over the study period. We can see that up to 20% wind forecast inaccuracy, the EENS is practically zero, due to about twice larger reserve amounts compared to the case when the entire load was served by conventional generation alone. This is a peculiarity of the system under study, which continues to commit a relatively large number of units that are lightly loaded even in the presence of abundant wind generation. This is due to the heat load schedules for CHP units, and minimum up- and down-time requirements and start-up costs for conventional units, which can be significant especially for large, coal-fired units. As a result, the system reserve (defined as the sum of the differences between installed capacity and scheduled MW for all conventional units) implicitly ends up much above the minimum reserve requirement. Not exactly cost-efficient but certainly very reliable. Only for the unusually high wind forecast inaccuracy of 40%, does the system with wind reach a comparable EENS with the system without wind.

TABLE I
RESERVE AND EENS FOR 3.5 DAYS UC-ED SCHEDULE

	Reserve (%)	EENS (%)
Load Only $\sigma_l = 4\%$	17.5	0.2
Load & Wind $\sigma_w = 10\%$	33.7	0.0
Load & Wind $\sigma_w = 20\%$	33.7	0.0
Load & Wind $\sigma_w = 40\%$	33.7	0.3

The time series for LOLE and system reserve levels are presented together for a 3.5 day simulation period in figure 9, for the base case (no wind, load served by conventional generation alone, 4% forecast inaccuracy) and the case of 8 GW installed wind capacity, with an associated 40% forecast inaccuracy. As expected, periods of lower reserve coincide with higher LOLE for both cases.

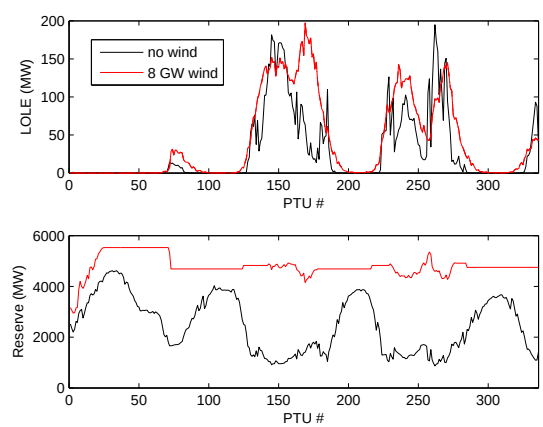

Fig. 9. LOLE and Reserve for 3.5 days Schedule, $\sigma_l = 4\%$ and $\sigma_w = 40\%$

V. CONCLUSION

A statistical interpolation method to generate time series of system-aggregated wind power production values has been developed in this paper. The method takes into account the spatial correlations among multiple sites, as derived from the measurement data. A confidence interval for the system-wide aggregated wind power production estimate was also derived. The method was used to get an idea of

the degree of variability introduced by large-scale wind production as compared to the inherent variations in customer demand, for a realistic power system. Moreover, the resulting wind power time series were used as an input to a system operations planning tool, namely Unit Commitment and Economic Dispatch, to determine commitment schedules and MW output levels for conventional units which were available for central dispatch. The effect of wind forecast inaccuracy on system-wide reliability indices such as LOLE and EENS was also investigated. Unfortunately, no feedback from this analysis back into the UC simulation tool was possible, so the effect of selective unit decommission and smaller reserve levels on system reliability could not be investigated.

As part of future work, the Monte Carlo simulation performed to determine EENS should be coupled with the simulation used to establish confidence intervals around the wind power production time series. Thus, the sensitivity of the system study to different wind power generation scenarios could be examined. In addition, it would be interesting to look at autocorrelative sampling from time series of net load forecast errors. Also, the incorporation of ramp rate constraints as a factor in reserve assessment for systems with large penetrations of wind energy would be a natural extension of the work presented here.

ACKNOWLEDGMENT

This research was partly funded under the framework of the Dutch Ministry of Economic Affairs BSIK program: 'Large-Scale Offshore Wind Power Generation', with support from the We@Sea consortium (www.we-at-sea.org). The authors would like to thank the Dutch Transmission System Operator TenneT (www.tennet.nl) and especially Eppie Pelgrum for providing valuable input. Also, use of data from KNMI – Royal Dutch Meteorological Institute – (www.knmi.nl) is acknowledged. Finally, Arno Brand of ECN (Energieonderzoek Centrum Nederland) should be thanked for incisive and detailed comments on the contents of this paper.

REFERENCES

[1] H. Wu, H.B. Gooi, "Optimal Scheduling of Spinning Reserve with Ramp Constraints," vol. 2. IEEE Power Engineering Society Winter Meeting, Feb. 1999, pp. 785–790.

[2] R. Billinton, R. N. Allan, *Reliability Evaluation of Power Systems*, 2nd ed. Plenum Press, 1996.

[3] R. Billinton, G. Bai, "Generating Capacity Adequacy Associated with Wind Energy," *IEEE Transactions on Energy Conversion, vol. 19, no. 3*, pp. 641–646, 2004.

[4] E.M. Gouveia, M.A. Matos, "Operational Reserve of a Power System with a Large Amount of Wind Power." 8th International Conference on Probabilistic Methods Applied to Power Systems, Iowa State University, 2004.

[5] R. Doherty, E. Denny, M. O'Malley, "System Operation with a Significant Wind Power Penetration." IEEE Power Engineering Society Annual Meeting, 2004.

[6] G. Dany, "Power Reserve in Interconnected Systems with High Wind Power Production." IEEE Porto Power Tech Conference, 2001.

[7] J. Verkaik, "A Method for the Geographical Interpolation of Wind Speed over Heterogeneous Terrain." [Online]. Available: http://www.knmi.nl/samenw/hydra/documents/geograph/index.html

[8] P.J. Brockwell, R.A. Davis, *Time Series: Theory and Methods*, 2nd ed. Springer, 1991.

[9] G. Giebel, *On the Benefits of Distributed Generation of Wind Energy in Europe*. Ph.D. Dissertation, Carl von Ossietzky University Oldenburg, 2000.

[10] L. Landberg, M.A. Hansen, K. Vesterager, and W. Bergstrom, "Implementing Wind Forecasting at a Utility," Risoe National Laboratory, Roskilde, Denmark, Tech. Rep. Riso-R-929(EN), 1997.

[11] J.F. Walker, N. Jenkins, *Wind Energy Technology*. Wiley, 1997.

[12] A.J. Brand, "Observed and Predicted Wind Speed Time Series in the Netherlands and the North Sea," Energie Centrum Nederland (ECN), Petten, The Netherlands, Tech. Rep. ECN-C–06-007, 2006.

[13] A.J. Brand, T. Hegberg, "Offshore Wind Atlas," Energie Centrum Nederland (ECN), Petten, The Netherlands, Tech. Rep. ECN-C-CX-04-136, 2004.

[14] B.C. Ummels, M. Gibescu, E. Pelgrum, W.L. Kling, "System Integration of Large-Scale Wind Power in the Netherlands." IEEE Power Engineering Society Annual Meeting, Montreal, Canada, 2006.

[15] G. J. Anders, *Probability Concepts in Electric Power Systems*. John Wiley & Sons, 1990.

[16] M. Shahidehpour, H. Yamin, Z. Li, *Market Operations in Electric Power Systems: Forecasting, Scheduling, and Risk Management*. Wiley-IEEE Press, 2002.

[17] J. Tambke, C. Poppinga, U. Gräve, L. von Bremen et al., "Forecasting Wind Power above North and Baltic Sea Using Combined and Refined Numerical Weather Predictions." Fifth International Workshop on Large-Scale Integration of Wind Power and Transmission Networks for Offshore Wind Farms, Glasgow, 2005.

[18] G. Giebel, "The State-Of-The-Art in Short-Term Prediction of Wind Power. A Literature Overview," EU Project ANEMOS, Tech. Rep. ENK5-CT-2002-00665, 2003. [Online]. Available: http://anemos.cma.fr.

[19] L. Söder, "Simulation of Wind Speed Forecast Errors for Operation Planning of Multi-Area Systems." 8th International Conference on Probabilistic Methods Applied to Power Systems, Iowa State University, 2004.

[20] U. Focken, M. Lange, K. Monnich, H.-P. Waldl, H.G. Beyer, A. Luig, "Short-Term Prediction of the Aggregated Power Output of Wind Farms – A Statistical Analysis of the Reduction of the Prediction Error by Spatial Smoothing Effects," *Journal of Wind Engineering and Industrial Aerodynamics*, vol. 90, pp. 231–246, 2002.

[21] L. Söder, "Reserve Margin Planning in a Wind-Hydro-Thermal Power System," *IEEE Transactions on Power Systems*, vol. 8, no. 2, pp. 1345–1354, 1993.

[22] H. Holttinen, "Optimal Electricity Market for Wind Power," *Energy Policy 33*, pp. 2052–2063, 2005.